Mannesmann piercing of ingots by plugs of different shapes

M. M. Skripalenko[1], V. E. Bazhenov*[1], B. A. Romantsev[1], M. N. Skripalenko[1], T. B. Huy[1] and Y. A. Gladkov[2]

The purpose of the research reported here was to establish how plug shape influences the size and porosity of hollow shells produced by Mannesmann piercing of an ingot. Ingots were cast from 6060 aluminium alloy and then pierced with a solid plug, a plug with a cavity or a hollow plug. Computer simulation of these processes was carried out using ProCast and QForm software and showed that a hollow plug should produce hollow shells with minimal porosity. However, the results of the experimental piercing revealed that the hollow plug in fact produced hollow shells with higher porosity than that of shells produced using either of the other two plugs. This appears to be consequence of the hollow plug losing stability.

Keywords: Mannesmann piercing, Plug, Shrinkage porosity, Hollow shell, Ingot casting, Computer simulation

Introduction

Continuing improvements in finite element method (FEM) simulation software open new prospects for studies of casting and metal-forming processes. In the investigation of metallurgical manufacturing processes, there is a significant current trend towards the combined use of several different software packages to design models that include as many processing steps as possible. Recent years have seen the publication of the results of a number of investigations in which different FEM software packages were applied. Jaouen *et al.*[1] used THERCAST and FORGE NXT (then called FORGE 3D) to simulate casting and forging of ingots. De Micheli *et al.*[2] applied FORGE to simulate a chain of metallurgical processes and to describe the evolution of ingot microstructure during metal-forming process. Using ProCAST and DEFORM-3D, Skripalenko *et al.*[3] simulated press piercing of ingot by piercers of different shapes and established how piercer shape affects the density of hollow shells. Ingot casting and forging were simulated by Abdullin and Ershov[4] using QForm and ProCAST. Romashkin *et al.*[5] simulated steel ingot forging with the help of the same software.

For casting simulation, computational fluid dynamics packages or specialised software such as ProCAST and Magma are used.[6–8] Casting simulation is mainly used to determine the distribution of shrinkage defects in ingots.[9] Simulations of stress and strain rate, grain structure and macrosegregation have been performed.[10,11] Simulation has also proved to be a useful tool to reveal the mould stress distribution during ingot casting.[12] The success of these various simulations has been shown by the good agreement between their results and those of experiments.

The ultimate objective of these simulations is to design models of metal-forming processes in which the plastic deformation characteristics are much more complex than those occurring during forging or pressing. Examples of such processes are Mannesmann rolling and piercing and the three-roll screw rolling process. The first of these exhibits a specific significant feature, namely the so-called 'Mannesmann effect', i.e. axial fracture of the billet during piercing and rolling, a detailed analysis and investigation of which (mainly through modelling) has been conducted by Ghiotti *et al.*[13] This phenomenon has also been modelled using different approaches, including the Galerkin method.[14]

The development of FEM software has prompted new investigations of Mannesmann rolling and piercing and of Assel rolling, using software designed by Transvalor. Chastel *et al.*,[15] with the help of Forge 2005, simulated Mannesmann rolling to determine how cracks appear and evolve. Pschera *et al.*[16] used Forge 2008 to detect zones in which plastic deformation reaches critical values during Mannesmann piercing. A FEM simulation was carried out by Kim *et al.*[17] to describe the features of deformation and the evolution of a microstructure during three-roll screw rolling of copper parts. Lopatin[18] applied LS-DYNA to investigate how hot screw rolling affects the microstructure of a titanium alloy. Along with DEFORM, Forge, QForm and other commercial software, LS-DYNA is one of the most commonly used in metal-forming research.[19] LS-DYNA was used by Lopatin[20] to study the evolution of the microstructure of pure titanium under warm forming during screw rolling and by Lopatin *et al.*[21] to study the formation of the globular structure during screw rolling of parts made of titanium alloy. Reggio *et al.*[22] described how plug shape

[1]National University of Science and Technology 'MISiS', Leninskiy pr. 4, Moscow 119049, Russia
[2]Quantorform, Limited Liability Company, Vtoroy Yuzhnoportoviy proezd 16, Building 2, Moscow 115088, Russia

*Corresponding author, email V.E.Bagenov@gmail.com

Published by Taylor & Francis on behalf of the Institute
Received 18 September 2015; accepted 19 January 2016
DOI 10.1080/02670836.2016.1145840

influences forming during Mannesmann piercing. Comparing the results of simulation with those of piercing experiments, Zhao *et al.*[23] demonstrated the effectiveness of simulation of Mannesmann piercing using DEFORM-3D. Pater *et al.*[24] presented a clear illustration of the effectiveness of MSC SuperForm 2005 for simulation of the tube-forming process in a Diescher mill. Another commercial software package whose utility has been demonstrated by comparison with laboratory skew rolling results is Simufact Forming 10.0. This software was used by Pater and Kazanecki[25] to estimate the effect of different parameters on the effective strain and temperature distribution of the billet and the distribution of the forces affecting tools during rotary piercing using a Diescher mill.

The conditions for closing voids during metal-forming process are of interest. The evolution of voids into cracks in an ingot was analysed in detail by Znang and Cui.[26] To simulate the forging of a steel ingot, taking account of shrinkage porosity, Chen *et al.*[27] added voids of cylindrical shape to a three-dimensional model and mesh. Lee *et al.*[28,29] made X-ray scans of internal voids and included them in the mesh to simulate forging with DEFORM-3D. Kim *et al.*[30] simulated the forging of a 520-ton ingot and carried out experimental forgings of lead billets to verify the model. The evolution of internal defects in ingots, including axial shrinkage porosity, was studied by Kikamoto *et al*.[31]

The results of these investigations have demonstrated that computer simulation using FEM software is an effective tool for the study, analysis and optimisation of screw rolling and piercing. Since ingots and continuously cast billets are widely used for the manufacture of hollow shells, it is important to consider the use of two different FEM software packages in combination, one for casting simulation and the other for forming simulation, to study the influence of plug shape on the process of forming of cast parts and the features of the products.

This paper reports on a study of the Mannesmann piercing of ingots both experimentally and through simulation using a computer model. The specific goal was to determine how the plug shape in Mannesmann piercing influences the density of hollow tube parts.

Materials and methods

Casting of ingots

Melting was carried out in a clay graphite crucible in a resistance furnace. Bars of 6060 aluminium alloy were used. The alloy was treated with Arsal 2125 refining flux and degassed with hexachloroethane. Ingots of 60 mm diameter and 210 mm height were manufactured. Alloy, at 740°C, was poured into a mould, preheated to 150°C, made of A356 aluminium alloy. Before pouring, the mould was covered by a gravity dye coating of Cillolin Al285. The alloy composition was determined using an ISP-30 optical emission spectrometer.

Table 1 Parameters for simulation of ingot casting

Parameter	Value
Mould filling time, τ	3 seconds
Heat transfer coefficient, *iHTC*	1000 W m^{-2} K^{-1}
Pouring temperature, t_{pour}	740°C
Mould temperature, t_{mould}	150°C
Alloy liquidus temperature, t_{liq}	654°C
Alloy solidus temperature, t_{sol}	608°C

Mannesmann piercing of ingots

Ingots were pierced using the MISIS-130D Mannesmann mill of the Tube Technology and Equipment Department, National University of Science and Technology. A schematic view of the numerically analysed piercing process in the Mannesmann mill is presented in Fig 1. For better visualisation, only one of the guiding shoes is shown in Fig. 1*a* and neither guide is included in Fig. 1*b*. The minimum gap between the rolls (usually called the 'draft') was 52 mm and the gap between the supporting shoes was 60.5 mm. The feed angle was 14° and the inclination angle of the rolls was 0°. The rolls were of length 300 mm and diameter 410 mm and the length of the draft section was 10 mm. The entry and exit tapers of the rolls were 3° and their rotational speed was 5.23 rev min^{-1}. Billets were preheated to 400°C. Three different plugs were used: a solid plug, a hollow plug and a plug with a cavity (Fig. 2).

Sections of 30 mm were cut from the hot top of the ingot before piercing. This was done in order to use the left part of the ingot's pipe to provide better centring of plugs during piercing.

Analysis of porosity of hollow shells

Traditionally, the shrinkage porosity of ingots is determined using macro-etching, ultrasound and dye penetration tests.[32] Here, the shrinkage porosity of the ingots and the porosity of the hollow shells were revealed using a metallographic method. Ingots and hollow shells were cut along their diameters into two halves. One-half of an ingot and one-half of a hollow shell were ground and polished. These metallographic samples were photographed and all the areas not corresponding to the image of the metallographic sample were deleted from the photographs. Visible voids were painted. Image Expert Pro 3 software was used and the percentage of the image area occupied by porosity, $S_{por.true}$ was calculated according to the following equation:

$$S_{por.true} = \frac{(S_{por.im} \cdot 100)}{S_{obj}} = \frac{(S_{por.im} \cdot 100)}{(100 - S_{bg})} \qquad (1)$$

where $S_{por.im}$ is the percentage of the area of the image occupied by porosity, S_{obj} is the percentage occupied by the section of the ingot or hollow shell and S_{bg} is the percentage occupied by background. Microstructural investigations were carried out by means of a TESCAN VEGA SBH 3 scanning electron microscope.

Computer simulation of ingot casting

Computer simulations of ingot casting were realised using ProCast software. The temperature dependence of thermal conductivity, density and enthalpy (Fig. 3), the solid fraction, and the alloy's liquidus and solidus temperatures (Table 1) were calculated using the ProCAST thermodynamic database (CompuTherm LLC Database for Al alloys). The accuracy of these thermodynamic calculations of thermal properties has been shown in several papers. In their work on reducing macrosegregation in steel ingots, Sang *et al.*[33] used thermal properties

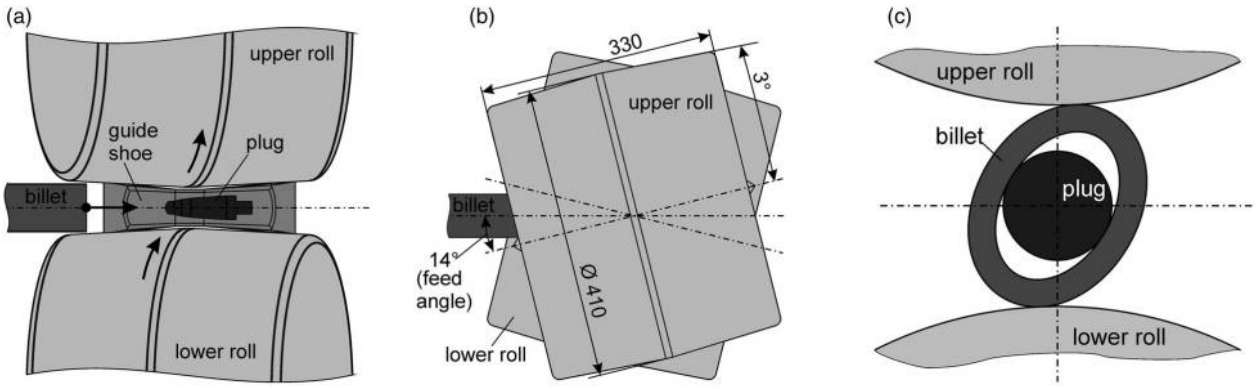

1 Schematic view of the numerically analysed Mannesmann piercing process: *a* side view; *b* top view; *c* cross-section of contact zone between rolls

calculated with the ProCAST thermodynamic database. Hartmann *et al.*[34] calculated thermal properties with the help of JMatPro. The simulation mesh had approximately 130 000 elements. The simulation parameters are listed in Table 1. The low value of the interfacial heat transfer coefficient is due to the presence of a significant layer of gravity dye. The value of the critical piping solid fraction PIPEFS was set to zero to allow porosity values to be obtained for all nodes of the mesh on completion of the simulation.

Simulation of Mannesmann piercing of ingots

The results of the ProCAST simulation, namely the mesh and porosity data, were loaded into QForm (Fig. 4). Then, in line with the experimental procedure, a 30 mm section was cut from the ingot in QForm.

The assembly for the simulation of billet piercing in the MISIS-130D Mannesmann mill is presented in Fig. 5. The input parameters for QForm were the same as the experimental parameters (see the subsection 'Mannesmann piercing of ingots'), including, among others, the billet temperature, the angular velocity of the rolls, the roll material and the billet material. The billet was initially heated throughout its volume to 400°C. The initial temperature of the tools was 20°C. The friction factor for the rolls was set to 1 in the Siebel friction law. The friction factors for the other tools, namely the plug and the guiding shoes, were all set to 0.8 in the Siebel friction law. The plug, guiding shoes and rolls were taken to be rigid bodies, i.e. they were subject to neither elastic nor plastic deformation during the simulation.

QForm provides an option for simulation of metal-forming process of porous materials. The effectiveness of using this option in the case of ingot forging was demonstrated by Abdullin and Ershov.[4] If a porous material undergoes forming during the simulation, there is a system of governing equations that the QForm software applies strictly in that case.[35] There is no need for users to write their own subroutines or to take any additional actions other than simply specifying during preprocessing that the billet material is porous.

Table 2 Chemical composition of alloy (wt-%)

Al	Mg	Si	Fe	Cu	Mn	Zn	Ti
Balance	0.35	0.48	0.5	0.1	0.09	0.11	0.08

Results and discussion

Ingot porosity

The chemical composition of the alloy is given in Table 2. It can be seen that for all elements except Fe, the alloy corresponds to the 6060 wrought alloy, which should contain only 0.1–0.3 wt-% Fe. The high Fe concentration of the alloy here may be connected with incorporation of Fe from the steel tools used in its preparation.

Figure 6*a* shows the simulated shrinkage porosity distribution, which can be compared with the diametral section of a cast ingot in Fig. 6*b*. It can be seen that the simulated ingot pipe shape (with a shrinkage porosity value of 60–100%) coincides almost exactly with that of the cast ingot. Shrinkage porosity is hardly visible in the diametral section in Fig. 6*b*, which is why it cannot be estimated quantitatively. Therefore, a specimen of size 30 mm × 15 mm was cut from the ingot and examined with a scanning electron microscope. Figure 6*c* shows a 5 mm × 5 mm area of the specimen from the centre of the ingot. It is significantly affected by shrinkage porosity. According to the results of Image Expert Pro 3 analysis, the shrinkage porosity in that area is 3.7%. Figure 6*d* shows a 5 mm × 5 mm area of the specimen 5 mm from the centre of the ingot. Here, the porosity appears to be considerably lower, at just 0.2%, although, under higher magnification, it is found that the porosity of this area is actually much higher. The microstructure of this area of the specimen is shown in Fig. 7. Thin voids can be seen along the boundaries of the dendritic cells. For the area of the specimen 5 mm from the centre of the ingot, the shrinkage porosity according to Fig. 7 was 1.1%. A comparison of simulated and experimental results for the porosity, from the ingot centre to its surface at a fixed height, is presented in Fig. 8. It is clear that the shrinkage porosity is greatest 0–5 mm from the ingot centre. The simulated and experimental results for porosity in that region differ dramatically. This may be due to inaccuracy in cutting the diametral section of the ingot. Another reason may be a radical change in the porosity of this region, in which case the simulation results would depend strongly on the tetrahedral mesh size. Starting at 5 mm distance from the ingot centre and outwards, the simulated and experimental values of the shrinkage porosity

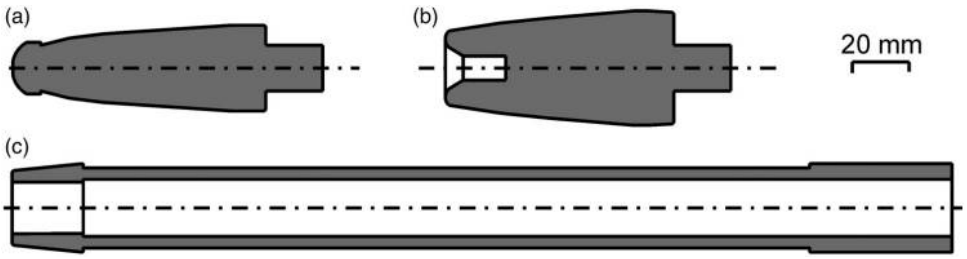

2 Plugs used for Mannesmann piercing: *a* solid plug; *b* plug with a cavity; *c* hollow plug

are almost equal. It can be inferred from this that the simulation results are satisfactory and that the ingot model, and its associated data, may be used for further simulation of the Mannesmann piercing process.

Shape and size of hollow shells

It has been established both experimentally and through simulations that during piercing by a hollow plug or a plug with a cavity, metal flows not only along the surface of the plug but also into it, forming a tail. The tails appearing in simulations of piercing by a hollow plug and a plug with a cavity have the same forms as those produced in experimental piercings (Fig. 9).

In simulations using QForm, the tails did not separate from the plugs. This was because the simulation results were expressed in terms of the billet density change during piercing and consequently a very thin metal layer appeared connecting the tail and the hollow shell of the plug (Fig. 9). In contrast, in the experiments, the tails became separated from the hollow shells. The most common operation after piercing is elongation in a mill with mandrel. For this, tails are undesirable and therefore they were cut off in the QForm simulations. With this option, the geometry of the hollow shells, the mesh and the data on the variables can be retained, allowing the process to be simulated further, including elongation on a mandrel, until a seamless tube has been obtained.

The dimensions of the hollow shells according to the simulation (after the tails had been removed in QForm) are compared with the experimental results in Figs. 10 and 11. The differences in diameter between simulation and experiment are estimated as no more than 2–3% and the differences in the lengths of the hollow shells are estimated as 9.4% for the hollow plug, 3.9% for the solid plug and 11.8% for the plug with a cavity.

Porosity of hollow shells

One of the key advantages of using ProCAST and QForm in combination is the option to estimate the influence of plug shape on forming and the generation of porosity in the hollow shells. It was found that there are differences in the intensity of consolidation of the hollow shells and in the areas in which it occurs (Figs. 12–14).

In contrast to the solid plug, for the hollow plug and the plug with a cavity, blocks of porosity (or low density) appear in the shells. This is because the metal filling the hollow plug or the cavity has a lower density than the metal in the walls. In both the simulated and experimental results for the hollow plug, there are easily recognisable voids (Figs. 9 and 13). In contrast, after piercing with the solid plug, the density of the tail is almost 100%.

A comparison of the porosity of shells pierced in the Mannesmann mill and the results simulated using QForm is shown in Fig. 15. For the QForm shells, the mean value of the porosity was calculated and was found to be 0.2% for a shell pierced by the hollow plug, 0.3% for a shell pierced by the plug with a cavity and 0.5% for a shell pierced by the solid plug.

Figure 15 shows the key results of this work and deserves further detailed discussion and analysis. Considering it independently of other results, both simulation and experiment show a common trend, namely that the porosity of a hollow shell pierced by the solid plug is higher than that of one pierced by the plug with a cavity. However, there are significant quantitative differences between simulation and experiment: 25% for piercing with the solid plug (0.67% from the experiment versus 0.5% from the QForm simulation) and 52% for piercing with the plug with a cavity (0.63% versus 0.3%). From a comparison of the results for all three plugs, it can be seen that the simulations do not reflect the trend revealed

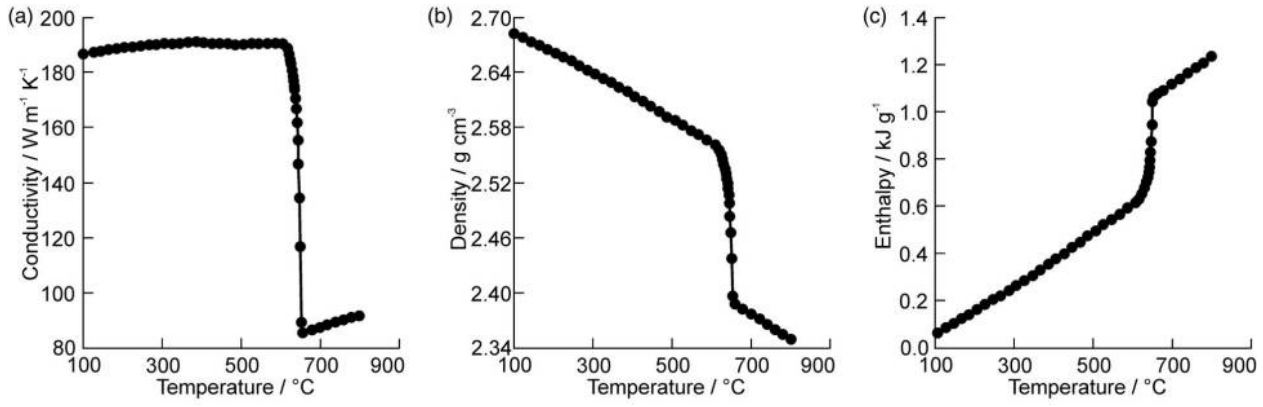

3 Thermal properties of the alloy: *a* thermal conductivity; *b* density; *c* enthalpy

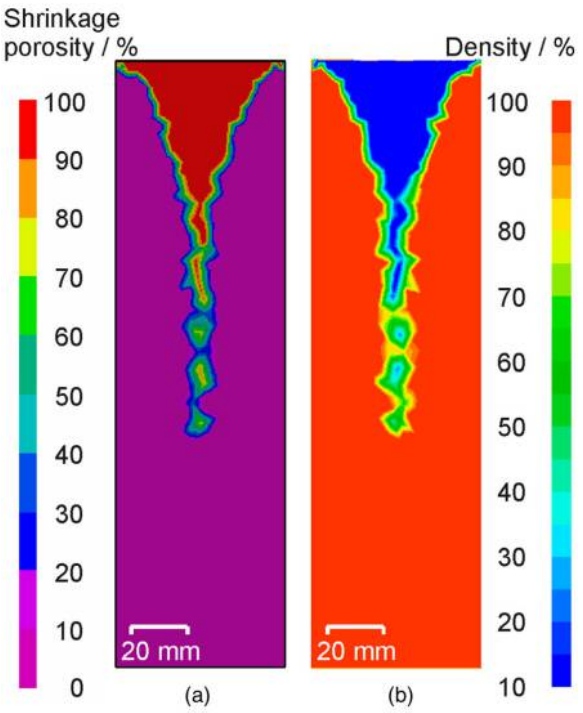

4 Shrinkage porosity of ingot in diametral section in a Pro-CAST and *b* QForm

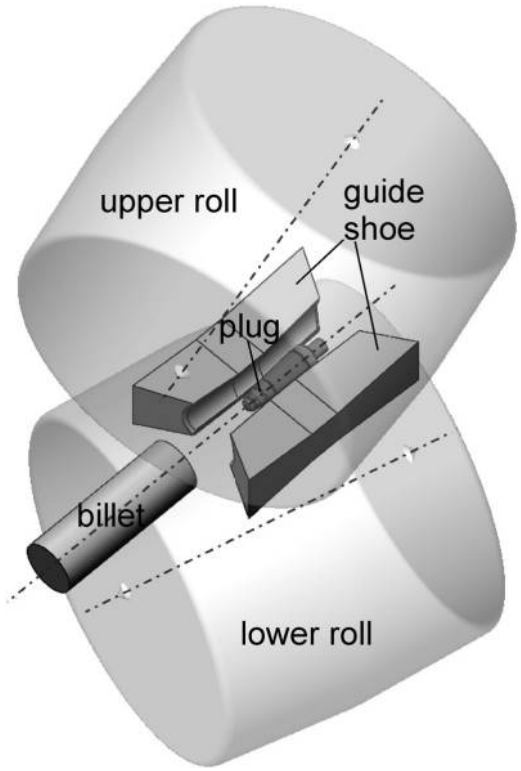

5 SolidWorks three-dimensional model for simulation of Mannesmann piercing

by experiment, according to which the porosity of the hollow shells produced with the different plugs decreases in the order hollow plug > solid plug > plug with a cavity. In contrast, according to the QForm simulations, the porosity decreases in the order solid plug > plug with a cavity > hollow plug. Indeed, the difference between the experimental and simulated results for the hollow plug is even greater than the differences for the solid plug and the plug with a cavity mentioned above, with the experimental value of the porosity being nearly nine times that given by the simulation (1.79% versus 0.2%).

According to Fig. 13, the hollow plug cuts out a volume with axial porosity, with metal retracting into the hole in

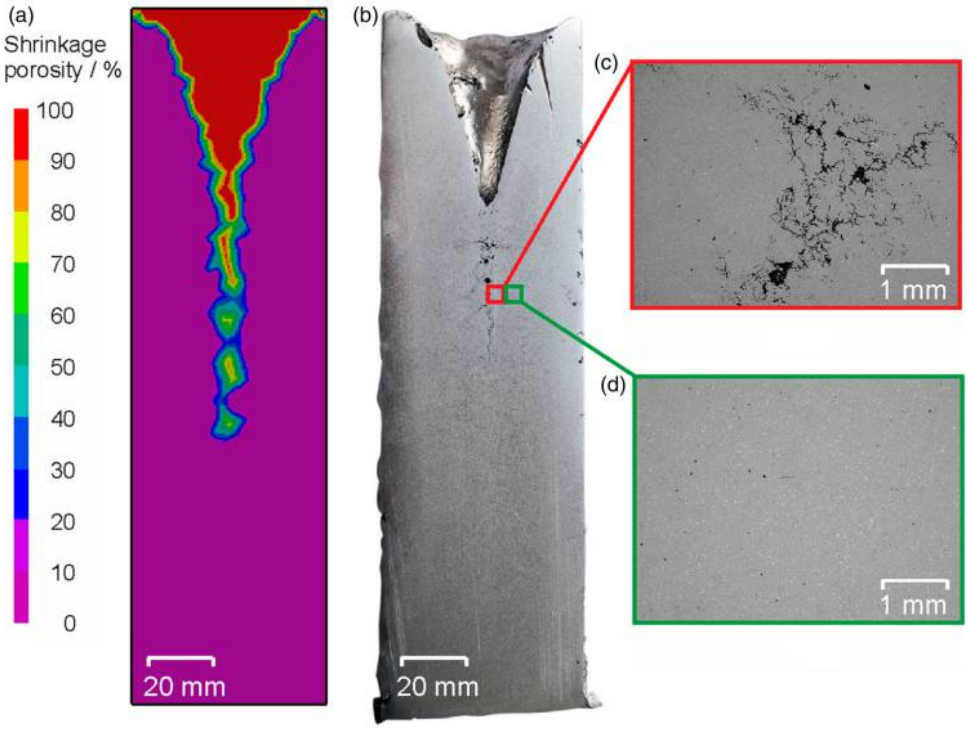

6 *a* shrinkage porosity of ingot obtained by ProCAST simulation; *b* photograph of cut billet; *c* and *d* SEM images showing microstructures of specimens cut from ingot

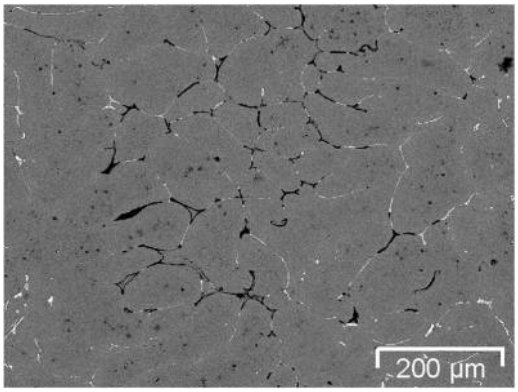

7 Shrinkage porosity in ingot specimen (SEM)

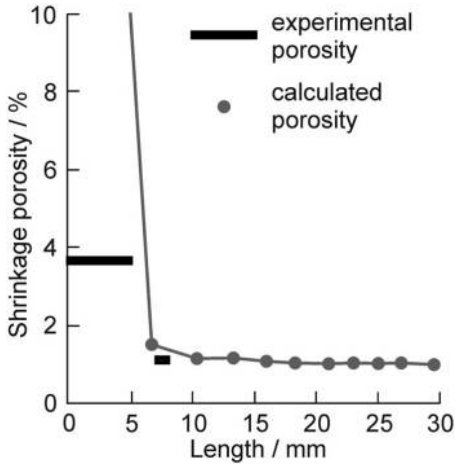

8 Calculated and experimental density distributions in ingot (the origin corresponds to the centre of the ingot)

the plug. It can be clearly seen that almost all the metal in the wall of the hollow shell has 100% density, with only very small 95% density areas at the edges. When the solid plug is used (Fig. 12), significant volumes of metal with density lower than 100% appear in the wall of the hollow shell, especially close to the edges. It can be assumed that when the plug with a cavity is used (Fig. 14), the density in the wall of the hollow shell is somewhere between the densities obtained with the solid and hollow plugs. When there is space remaining in the cavity, this plug acts as if it were hollow. However, once the cavity has filled completely with metal, the plug acts like a solid plug and volumes with density lower than 100% appear in the wall of the hollow shell.

The discrepancy between simulated and experimental results in Fig. 15 may be due to differences between the conditions assumed in the QForm simulation and the experimental piercing conditions. The inner surface of a hollow shell pierced by the hollow plug (Fig. 11*a*) exhibits a waviness with a clear periodic character, whereas for the other hollow shells (Fig. 11*b* and *c*) no such phenomenon occurs. It can be concluded from this that the hollow plug was vibrating while piercing, which could be explained by the features of its construction: it is much longer than the solid plug and the plug with a cavity. In addition, because this plug is fixed to a special bar, the total length of the hollow plug plus bar is considerably greater than the lengths of the solid plug and the plug with a cavity. Therefore, during Mannesmann piercing, the hollow plug vibrates much more and is less stable than the other plugs and therefore produces a wavy pattern on the inner surface of the hollow shell. For the same reason, the hollow shell pierced by the hollow plug is the shortest and has the thickest wall (11–14.5 mm for the hollow plug, 11–12.5 mm for the solid plug and 10–11 mm for the plug with a cavity). In other words, the draw value after experimental Mannesmann piercing with the hollow plug is the lowest, even though the hollow plug and the solid plug have the same diameter, 32 mm (the plug with a cavity has diameter 39 mm). Owing to the reduced stability of the hollow plug, the forming of the metal of the ingot was poor, resulting in a higher porosity of the hollow shell than when the other plugs were used.

In the QForm simulation, all the plugs were considered as rigid objects with fixed positions. In contrast to the experimental results, the simulation predicts the same wall thickness of the hollow shell when either the hollow

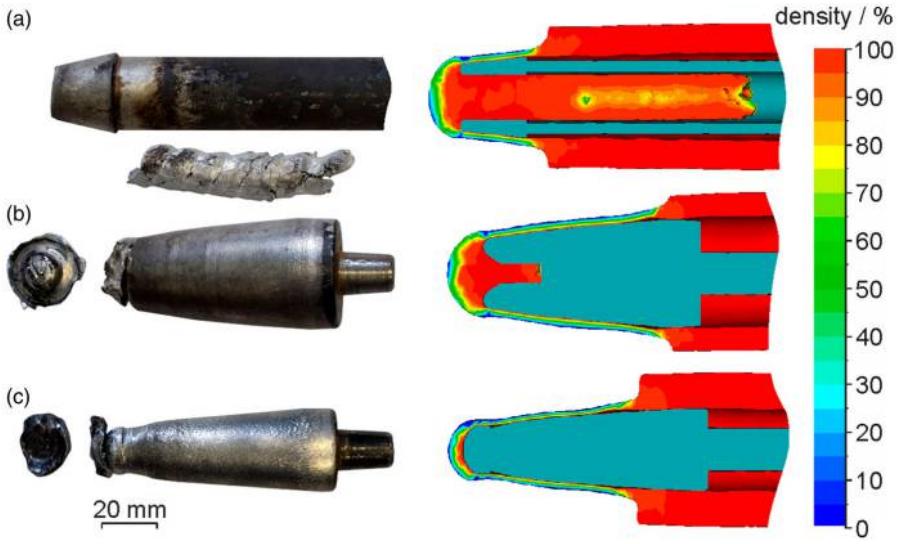

9 Tails after experimental Mannesmann piercing (left) and QForm simulation (right): *a* after piercing by hollow plug; *b* after piercing by plug with cavity; *c* after piercing by solid plug

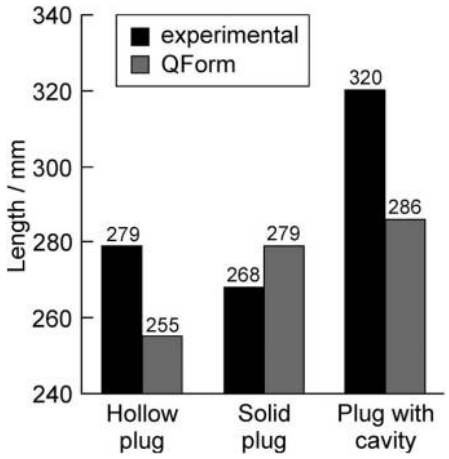

10 Lengths of hollow shells after experimental Mannesmann piercing and simulation in QForm

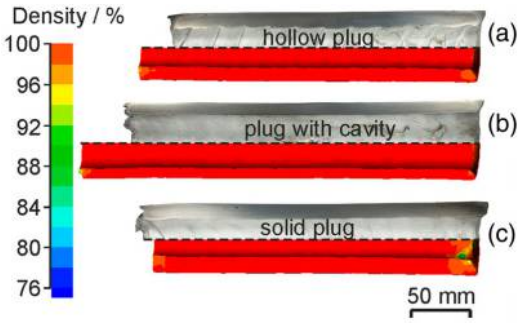

11 Comparison of porosity and size of hollow shells after experimental Mannesmann piercing and after QForm simulation (diametral section): *a* pierced by hollow plug; *b* pierced by plug with cavity; *c* pierced by solid plug

or solid plug is used: for both plugs, the thickness is 11–12 mm. According to the QForm simulation, with the plugs taken to be rigid and fixed, the density of the hollow shell

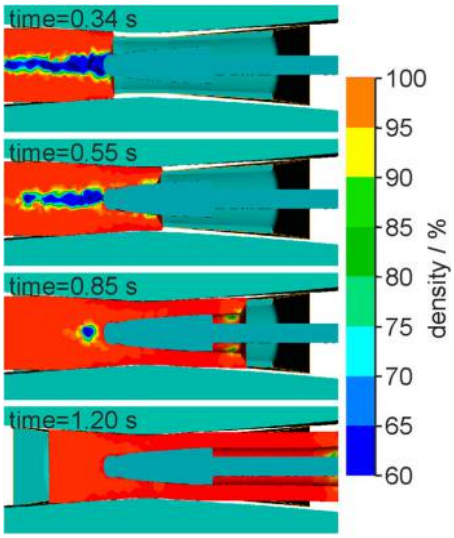

12 Density of billet at different stages of piercing by solid plug

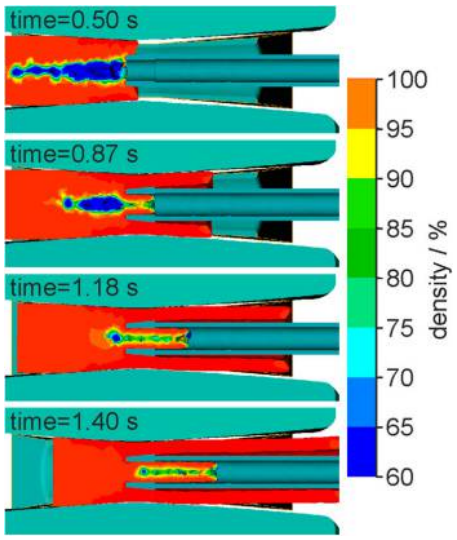

13 Density of billet at different stages of piercing by hollow plug

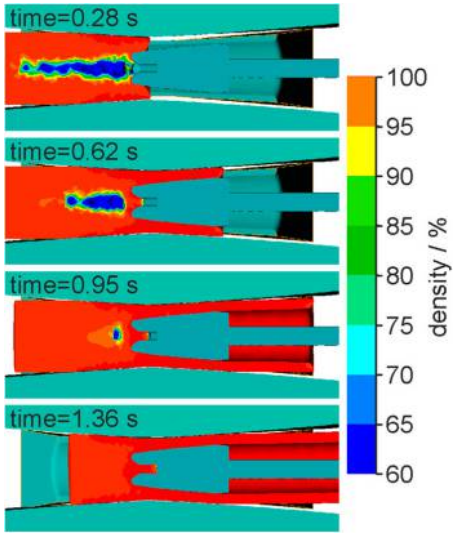

14 Density of billet at different stages of piercing by plug with cavity

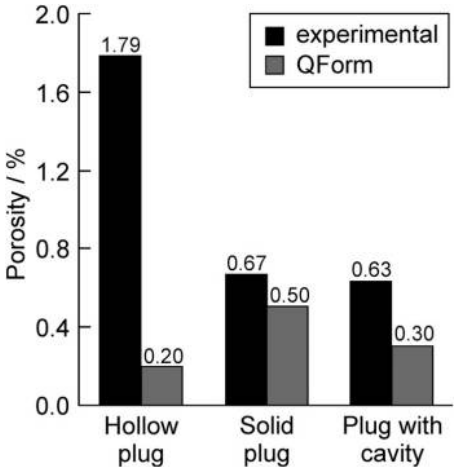

15 Comparison of porosity of hollow shells after experimental Mannesmann piercing and after QForm simulation

is higher when the hollow plug is used than when either the solid plug or the plug with a cavity is used (Figs. 12–14). The results obtained here suggest that if the hollow plug can be redesigned to reduce its level of vibration, this will allow the production of shells with the highest density (or with minimal porosity).

The elimination of density variations during metal-forming process is of great importance because such variations lead to anisotropic properties and increase the probability of increased stress, both of which are undesirable effects in terms of the quality of the final metal product.

The use of models like those considered here provides investigators with an additional tool to improve current metallurgical manufacturing technologies and to develop new ones involving metal-forming process of ingots and cast billets.

Conclusions

The investigations reported here involved the casting of 6060 aluminium alloy ingots and Mannesmann piercing of these ingots using different plugs. Computer simulations of the casting and piercing processes were performed using ProCAST and QForm software. The porosity values of hollow shells were determined both experimentally and from the simulations. The conclusions based on the results of these investigations can be summarised as follows:

i. Mannesmann piercing of ingots by a hollow plug or a plug with a cavity is feasible and offers a route to the manufacture of seamless tubes with minimal porosity.

ii. According to the simulated results, the lengths of the hollow shells produced using a hollow plug, a solid plug and a plug with a cavity were 255, 279 and 286 mm, respectively, whereas the corresponding experimental results were 279, 268 and 320 mm. The simulated results for the porosity of the hollow shells were 0.2%, 0.5% and 0.3% for the hollow plug, the solid plug and the plug with a cavity, respectively, whereas the corresponding experimental results were 1.79%, 0.67% and 0.63%. Comparing the use of the solid plug and the plug with a cavity, it can be seen from these results that, from both the simulation and the experiment, (a) the length of the hollow shell is greater for the plug with a cavity than for the whole plug and (b) the porosity of the hollow shell is higher for the solid plug than for the plug with a cavity. For both the length and the porosity of the hollow shell produced using the hollow plug, there are significant differences between the simulated and experimental results, which are particularly dramatic in the case of the porosity. It appears that these differences result from the assumption made in the simulation that the hollow plug was rigid and fixed, whereas, in reality and in contrast to the other plugs, it vibrated during piercing and exhibited a loss of stability. Thus, if this problem of vibration and instability can be overcome by suitable redesign of the hollow plug construction, it should be possible to produce hollow shells and seamless tubes with minimal porosity.

iii. Computer simulation allowed determination of the differences in the way the different plugs affect the axial porosity zones of pierced billets. The hollow plug, owing to flow of metal within its hole, is better than the other plugs at preventing the appearance of area of high porosity in the wall of the hollow shell. With the solid plug, clearly visible areas of high porosity appear in the wall of the shell. The plug with a cavity is intermediate between the other two in this respect: while metal is flowing into the cavity, it acts like the hollow plug, but when the cavity has completely filled with metal, it acts like the solid plug.

iv. The use of ProCAST and QForm software has provided a means to realise so-called multidomain simulation, introduced by the ESI Group. The approach used in the simulations described here provides opportunities for casting and metal-forming specialists to carry out joint investigations.

Acknowledgements

The authors wish to thank QUANTORFORM for their support for this research. One of the authors (M.M. Skripalenko) is grateful to Mr Arthur Gartvig for useful discussion and for consultations on numerical simulation.

ORCID

V. E. Bazhenov http://orcid.org/0000-0003-3214-1935

References

1. O. Jaouen, F. Costes, and P. Lasne: 'A new 3D simulation model for complete chaining casted and forged ingot', *Proc. 1st Int. Conf. on 'Ingot Casting, Rolling and Forging', Aachen, Germany*, 2012, 1–9.
2. P. De Micheli, A. Settefrati, S. Marie, J. Barlier, and P. Lasne: 'Towards the simulation of the whole manufacturing chain processes with FORGE®', *Proc. Int. Conf. on 'New development in forging technology', Stuttgart, Germany*, 2015, 1–25.
3. M. M. Skripalenko, V. E. Bazhenov, B. A. Romantsev, M. N. Skripalenko, A. V. Koltygin, and A. A. Sidorov: 'Computer modeling of chain processes in the manufacture of metallurgical products', *Metallurgist*, 2014, 58, 86–90.
4. A. D. Abdullin and A. A. Ershov: 'End-to-end simulation of casting and metal-forming operations with ProCAST and QForm software', *Metallurgist*, 2014, 58, 339–345.
5. A. N. Romashkin, V. S. Dub, I. A. Ivanov, S. I. Markov, A. N. Mal'ginov, and D. S. Tolstykh: 'Development of an integral production process for manufacturing machinery billets based on computer simulation', *Metallurgist*, 2015, 58, 821–830.
6. J. Li, M. Wu, A. Ludwig, and A. Kharicha: 'Simulation of macrosegregation in a 2.45-ton steel ingot using a three-phase mixed columnar-equiaxed model', *Int. J. Heat Mass Transfer*, 2014, 72, 668–679.
7. M. Tkadlečková, K. Michalek, K. Gryc, B. Smetana, P. Machovčák, and L. Socha: 'The effect of boundary conditions of casting on the size of porosity of heavy steel ingot', *J. Achiev. Mater. Manuf. Eng.*, 2013, 56, 29–37.
8. M. Heidarzadeh, H. Keshmiri, G. R. Ebrahimi, and H. Arabshahi: 'Influence of mould and insulation design on soundness of tool steel ingot by numerical simulation', *Int. J. Sci. Adv. Technol.*, 2011, 1, 37–40.
9. P. Zhang, X. Li, X. Zang, and F. Du: 'Optimizing casting parameters of steel ingot based on orthogonal method', *J. Cent. South Univ. Technol.*, 2008, 15, 296–300.
10. M. Ahmadein, M. Wu, and A. Ludwig: 'A novel technique for reducing macrosegregation in heavy steel ingots', *J. Cryst. Growth*, 2015, 417, 65–74.
11. J. P. Gu and C. Beckermann: 'Simulation of convection and macrosegregation in a large steel ingot', *Metall. Mater. Trans. A*, 1999, 30, 1357–1366.
12. P. Lan and J. Zhang: 'Study on the mechanical behaviors of grey iron mould by simulation and experiment', *Mater. Des.*, 2014, 53, 822–829.
13. A. Ghiotti, S. Fanini, S. Bruschi, and P. F. Bariani: 'Modelling of the Mannesmann effect', *CIRP Ann. Manuf. Technol.*, 2009, 58, 255–258.

14. S. Chiluveru: 'Computational modeling of crack initiation in cross-roll piercing', PhD thesis, Massachusetts Institute of Technology, MA, USA, 2007, 1–89.
15. Y. Chastel, A. Diop, S. Fanini, P. O. Bouchard and K. Mocellin: 'Finite element modeling of tube piercing and creation of a crack', *Int. J. Mater. Form.*, 2008, 1, 355–358.
16. R. Pschera, J. Klarner, C. Sommitsch: 'Modelling the forming limit during cross-rolling of seamless pipes using a modified continuum damage mechanics approach', *Steel Res. Int.*, 2010, 81, 686–690.
17. S. H. Kim, E. S. Park, M. Y. Huh, H. J. Kim, J. C. Bae: 'Evolution of strain states and microstructures during three-roll screw rolling of copper rods', *Trans. Mater. Process.*, 2008, 17, 68–72.
18. N. V. Lopatin: 'Effect of hot rolling by screw mill on microstructure of a Ti-6Al-4V titanium alloy', *Int. J. Mater. Form.*, 2013, 6, 459–465.
19. M. M. Skripalenko and M. N. Skripalenko: 'On choosing software for simulating metal-forming processes', *Metallurgist*, 2013, 57, 3–7.
20. N. V. Lopatin: 'Microstructure evolution in pure titanium during warm deformation by combined rolling processes', *Mater. Sci. Eng. A*, 2012, 556, 704–715.
21. N. V. Lopatin, G. A. Salishchev and S. P. Galkin: 'Mathematical modeling of radial-shear rolling of the VT6 titanium alloy under conditions of formation of a globular structure', *Russ. J. Non-Ferrous Met.*, 2011, 52, 442–447.
22. M. Reggio, F. McKenty, F. Gravel, J. Cortes, G. Morales and M.-A. Ladron de Guevara: 'Computational analysis of the process for manufacturing seamless tubes', *Appl. Therm. Eng*, 2002, 22, 459–470.
23. Y. Q. Zhao, J. H. Mao, F. F. Liu and Z. H. Ma: 'Experiments and simulation on Mannesmann piercing process in the drill steel manufacture', *Appl. Therm. Eng.*, 2015, 47, 29–40.
24. Z. Pater, J. Kazanecki and J. Bartnicki: 'Three dimensional thermo-mechanical simulation of the tube forming process in Diescher's mill', *J. Mater. Process. Technol.*, 2006, 177, 167–170.
25. Z. Pater, J. Kazanecki: 'Complex numerical analysis of the tube forming process using Diescher mill', *Arch. Metall. Mater.*, 2013, 58, 717–724.
26. X. Zhang and Z. Cui: 'Theoretical study of void closure in nonlinear plastic materials', *Appl. Math. Mech. (Engl. Ed.)*, 2009, 30, 631–642.
27. K. Chen, Y. Yang, K. Liu and G. Shao: 'Simulation of void defect evolvement during the forging of steel ingot', *Adv. Mater. Res.*, 2010, 97–101, 3079–3084.
28. Y. S. Lee, Y. C. Kwon, Y. N. Kwon, J. H. Lee, S. W. Lee and N. S. Kim: 'Analysis on void closure behavior during hot open die forging', *Adv. Mater. Res.*, 2007, 26–28, 69–72.
29. Y. S. Lee, S. U. Lee, C. J. Van Tyne, B. D. Joo and Y. H. Moon: 'Internal void closure during the forging of large cast ingots using a simulation approach', *J. Mater. Process. Technol.*, 2011, 211, 1136–1145.
30. Y. D. Kim, J. R. Cho and W. B. Bae: 'Efficient forging process to improve the closing effect of the inner void on an ultra-large ingot', *J. Mater. Process. Technol.*, 2011, 211, 1005–1013.
31. H. Kakimoto, T. Arikawa, Y. Takahashi, T. Tanaka and Y. Imaida: 'Development of forging process design to close internal voids', *J. Mater. Process. Technol.*, 2010, 210, 415–422.
32. M. Heidarzadeh and H. Keshmiri: 'Influence of mould and insulation design on soundness of tool steel ingot by numerical simulation', *J. Iron Steel Res. Int.*, 2013, 20, 78–83.
33. B. Sang, X. Kang and D. Li: 'A novel technique for reducing macro-segregation in heavy steel ingots', *J. Mater. Process. Technol.*, 2010, 210, 703–711.
34. L. Hartmann, C. Ernst and J.-S. Klung: 'Simulation of ingot casting processes at Deutsche Edelstahlwerke GmbH', *IOP Conf. Ser.: Mater. Sci. Eng.*, 2012, 27, 1–6. Article ID 012063.
35. '2015 QForm V8 Simulation Suite, QUANTORFORM', http://www.qform3d.ru.